THE ASTROPHYSICAL JOURNAL, 343:94–106, 1989 August 1

NEUTRAL HYDROGEN IN THE M96 GROUP: THE GALAXIES AND THE INTERGALACTIC RING

STEPHEN E. SCHNEIDER
Five College Astronomy Department, and Department of Physics and Astronomy, University of Massachusetts
Received 1988 September 26; accepted 1989 January 16

ABSTRACT

The M96 group is examined at 21 cm to study the galaxies' neutral hydrogen content and to search for evidence of interactions that might help explain the origin of the large intergalactic H I feature found there. M96, an Sab spiral, has 90% of its H I concentrated outside of the central bright optical disk—possibly captured intergalactic gas. The ringlike distribution of the intergalactic gas may, in turn, be shaped by interactions with M96. An extremely faint ($B \sim -10$ or -11) dwarf irregular galaxy was also found. Questions about the distance and membership of the M96 group are addressed, and it is shown that many previous group catalogs must be in error. A mass-to-light ratio of less than 30 is found for the M96 group; a number of previous estimates are inflated by inclusion of background galaxies—a problem that may be widespread in group studies. In the appendix, it is shown that a hexagonal (or "honeycomb") observing grid yields more optimized spatial frequency coverage than a rectangular grid.

Subject headings: galaxies: clustering — galaxies: intergalactic medium — radio sources: 21 cm radiation

I. INTRODUCTION

Small groups of galaxies provide an opportunity to observe several galaxies at the same distance in a relatively undisturbed environment. As such, groups have played an important role in studying the extragalactic distance scale and the halo masses of galaxies. These studies have generally been statistical in nature, because of the uncertainties of group membership and the lack of full three-dimensional information about the positions and velocities of the galaxies. However, the M96 group with its ring of intergalactic gas is uniquely suited for examining these issues without the usual uncertainties.

The key to this paper is a set of H I observations of the individual galaxies and of the entire M96 group region. The ring of intergalactic gas (Schneider 1985; Schneider *et al.* 1989; hereafter Papers I and II, respectively) permits a direct estimate of the mass of the central two galaxies in the group and suggests that relatively little extra mass is distributed far away from their optical images. M96 itself is interacting directly with the ring of gas and appears to be accreting gas from it; this impression is reinforced by H I synthesis observations which show that 90% of the neutral gas in M96 lies outside its visually bright disk.

In addition to demonstrating that no other intergalactic gas is present in the M96 group, a survey of the entire region of the group at 21 cm (Paper II) also provided a means of searching for optically faint galaxies which contain H I. One very faint dwarf irregular galaxy was discovered in this way, and follow-up CCD observations are presented here.

The M96 group is an important link in the extragalactic distance scale since it is the nearest group with both giant elliptical and spiral galaxies. It is a fairly compact group and the nearest of de Vaucouleurs's (1975*a*) groups with a preponderance of early-type galaxies. The boundaries of the group are disputed thanks to the complexity of the Leo region of galaxies. For example, NGC 3389 is a peculiar galaxy apparently lying within the intergalactic ring, making it a suspicious character among the galaxies in the neighborhood, but its redshift is relatively high, and the various group-finding methods disagree about whether it belongs to the M96 group.

The membership of the M96 group and the Leo region in general is reviewed here, and arguments in favor of a very limited membership are presented. The implication of the limited membership and of the intergalactic ring's orbital dynamics is that the mass-to-light ratio for the M96 group is considerably smaller than many previous studies have suggested, and the same arguments may apply to other groups as well.

Background information about the galaxies in the M96 group is reviewed in § II. H I observations made at Arecibo[1] of the three brightest spiral galaxies in the region are presented in this paper, together with a VLA[2] map of M96. The complementary aspects of Arecibo's good sensitivity and spectral resolution with the VLA's high spatial resolution provide a fuller understanding of the extension of gas from the intergalactic cloud complex toward M96. Sections III, IV, and V detail the H I observations of M96, along with observations of M95, NGC 3389, and other galaxies in the M96 region. The Arecibo H I detection of the faint dwarf galaxy and follow-up Kitt Peak[3] CCD observations are detailed in § VI. Finally, in §§ VII and VIII, group membership, dynamics, and questions of dark matter are reexamined in the context of the neutral hydrogen observations.

II. THE M96 REGION

The M96 group was identified by de Vaucouleurs (1975*a*) as a major condensation in the Leo I Cloud, and the 11th nearest group (G11) in his nearby-group catalog. It is notable as the nearest group with giant ellipticals (M105 = NGC 3379 and NGC 3377), lenticulars (NGC 3384 and 3412), and spirals

[1] The Arecibo Observatory is part of the National Astronomy and Ionosphere Center, which is operated by Cornell University, under contract with the National Science Foundation.

[2] The Very Large Array is part of the National Radio Astronomy Observatory, which is operated by Associated Universities, Inc., under contract with the National Science Foundation.

[3] Data obtained under the Observing Service Program of the Kitt Peak National Observatory, National Optical Astronomy Observatories, operated by the Association of Universities for Research in Astronomy, Inc., under contract with the National Science Foundation.

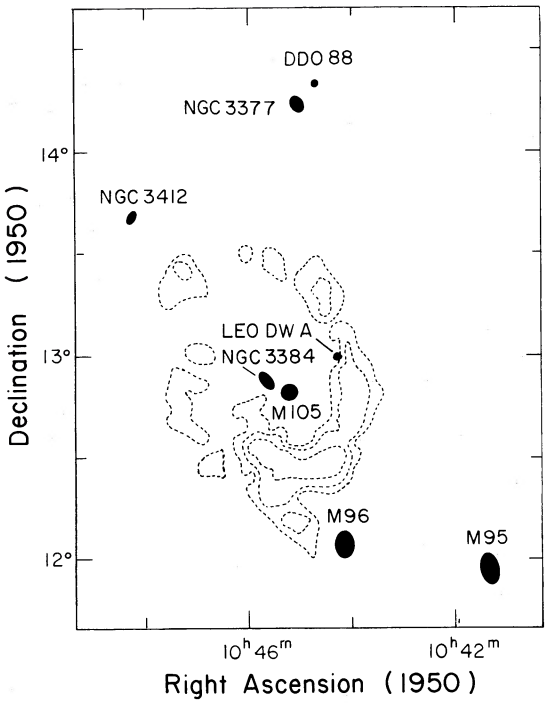

FIG. 1.—The inner region of the M96 group. The positions and approximate optical dimensions are shown for members of the M96 group in the vicinity of the intergalactic ring, the H I contours of which are shown with dashed lines (Paper II).

(M96 = NGC 3368 and M95 = NGC 3351), as well as several possible dwarf irregular members. de Vaucouleurs distinguishes the M96 group from the M66 Group (G9) ~10° to the east, which is slightly closer and includes the Leo Triplet, and he does not include some higher redshift galaxies, such as NGC 3389, based on independent distance estimators (de Vaucouleurs 1967). A general discussion of the Leo region and M96 group is included in Materne (1978). Isophotometry of many members of the M96 group is given by Dickson and Hodge (1981) and by Schanberg (1973).

In the course of a 21 cm redshift survey of possible group members, a large cloud of intergalactic neutral hydrogen was discovered between M96 and M105 (Schneider *et al.* 1983). Subsequent observations (Papers I and II) showed that the original H I cloud was the southern part of a ~200 kpc diameter ring surrounding M105 and NGC 3384. The central region of the M96 group, showing the position of the intergalactic ring of hydrogen, is illustrated in Figure 1. Only the galaxies with Galactocentric velocities (de Vaucouleurs, de Vaucouleurs, and Corwin 1976) between 400 and 900 km s^{-1} in the vicinity of the intergalactic ring are displayed.

For reference in the remainder of the paper, various parameters of M96, the intergalactic ring, and nearby galaxies, are collected in Table 1. All galaxies with Galactocentric velocities below 1600 km s^{-1} are listed out to a distance of 3° from M96. The galaxies are grouped by brightness into two distinct redshift domains which appear to correspond to at least two distinct groups along this line of sight (see §§ VII and VIII). The common name of the galaxy is given in column (1). Unless noted, its type in column (2) and B_T magnitude in column (3) are drawn from de Vaucouleurs, de Vaucouleurs, and Corwin (1976) when available and from Nilson (1973) otherwise, and

TABLE 1

PARAMETERS OF THE INTERGALACTIC GAS AND GALAXIES

Galaxy (1)	Type (2)	B_T° (3)	v_0 (km s^{-1}) (4)	w_{50} (km s^{-1}) (5)	$\int S_{HI}\,dv$ (Jy km s^{-1}) (6)	M_{HI} ($10^9\,M_\odot$) (7)	M_{dyn} ($10^9\,M_\odot$) (8)	L_c ($10^9\,L_\odot$) (9)
Intergalactic ring			700	280	70.9	1.67	640	<0.15?
M96	(R)SAB(rs)ab	9.8	757	338	89.5	2.11	200	19.
M105	E1	10.0	793[a]	214[b]	<1.2[c]	<0.03	260	16.
M95	SB(r)b	10.2	649	268	47.1	1.11	94	13.
NGC 3384	SB(s)0⁻	10.7	600[a]	157[b]	<0.8[d]	<0.02	68	7.7
NGC 3377	E5–6	10.9	567[a]	151[b]	<1.7[c]	<0.04	98	6.5
NGC 3412	SB(s)0°	11.2	731[a]	126[b]	<0.7[d]	<0.02	49	4.8
NGC 3299	SAB(s)dm	13.0?	465[e]	158	4.3	0.10	27	0.9
DDO 88	SAB(s)m	13.2?	449[e]	71	6.9	0.16	5	0.7
UGC 5812	I m	15.5[f]	876	55	1.5	0.04	1.7	0.15
Leo dw A	I m	18.9	510	28	0.3	0.008	0.05	0.005
NGC 3338	SA(s)c	11.0	1178[g]	337	126.1	7.60	249	14.
NGC 3389	SA(s)c	12.0	1169	263	27.7	1.66	46	5.8
UGC 5832	SB?	12.8?	1089	99	5.1	0.31	23	2.8
UGC 6014	SABdm	13.8?	991	84	2.3	0.14	4.8	1.1
Zw 066.029	Sm + Im?[f]	14.0[f]	1251	73	2.6	0.16	1.8	0.90
Mrk 1263	BCD?[f]	15.5[f]	1194	125	4.4	0.26	1.4	0.22

[a] Velocity from Huchra *et al.* 1983.

[b] Velocity dispersions and dynamical masses for E and S0 galaxies from Tonry and Davis 1981 adjusted to a distance of 10 Mpc. They note that their derivation of the dynamical mass applied to S0's is not entirely appropriate because the disk has not been modeled.

[c] Upper limits from Knapp, Kerr, and Williams 1978.

[d] Upper limits from Giovanardi, Krumm, and Salpeter 1983.

[e] Fisher and Tully 1981. Widths are measured at 20% of maximum.

[f] Hoffman *et al.* 1987. These magnitudes are based on visual estimates.

[g] Helou *et al.* 1981.

are corrected as in Schneider *et al.* (1986). The Galactocentric velocities are listed in column (4). H I velocity widths and optical dispersions are listed in column (5). The integrated H I fluxes, masses, and luminosities in columns (6)–(9) assume nominal distances to the M96 and background group of 10 and 16 Mpc respectively. The dynamical mass in column (8) is calculated as in Schneider *et al.* (1986) from inclination-corrected rotational properties out to the Holmberg radius. The dynamical mass associated with the intergalactic ring's orbit is adopted from Paper I, and the upper limit on the luminosity of the intergalactic ring in column (9) is extrapolated from measurements in Paper II.

The derived dynamical masses in Table 1 show that M105 is probably the dominant galaxy in the M96 group. Its magnitude is slightly fainter than M96's, but there is some uncertainty in the corrections applied. M105 is a more likely candidate for being the most massive galaxy, given its location central to the group and the intergalactic ring.

III. M96

M96 (NGC 3368) is an Sab spiral and is the brightest galaxy in the western half of the Leo region. Optically, M96 has a fairly normal structure for an Sab galaxy, with a high surface brightness 2.'8 × 1.'7 disk at position angle 145°, but it is surrounded by a much fainter ring or pair of arms extending to 7.'5 × 5.'0 at position angle 5°, so that the outer disk is shifted by ~40° relative to the inner disk. (For photographs, see Schanberg 1973, or The Hubble Atlas; Sandage 1961.) M96 is classified as (R)SAB(rs)ab by de Vaucouleurs and de Vaucouleurs (1964, including information in their notes). Outer ring structures are uncommon, occurring in only ~4% of all galaxies, but they are more common among early-type galaxies with a frequency of ~10%–15% in Sa and Sab galaxies (de Vaucouleurs 1975*b*). Even in The Hubble Atlas several other galaxies can be found that have a similar morphology, such as M77 (NGC 1068) and M94 (NGC 4736). Otherwise, M96 has not received much detailed study.

a) Arecibo H I *Observations*

M96 was mapped in H I at Arecibo using the linear polarization "flat" feed. This feed minimizes the problems of sidelobe confusion, which is especially important for examining the region just outside M96's disk where an extension of the intergalactic H I cloud approaches the galaxy.

Positions were observed every 3.'8 on a hexagonal grid. This observing pattern provides complete coverage of the emission with nearly uniform sensitivity in the minimum amount of time, although it does not fully sample the spatial frequency structure accessible to the Arecibo telescope. (See Appendix.) A 5 MHz bandpass was used in total power mode. After Hanning smoothing, the resolution was ~4 km s^{-1} and the noise was typically ~5 mJy. Most of the Arecibo spectra of M96 were collected in 1983 and 1984, while some additional spectra of this and other galaxies in the region have been obtained up through 1987. Further details about the flat feed can be found in Corbelli, Schneider, and Salpeter (1989).

The emission from M96, based on the sum of spectra covering a ~17′ diameter region centered on M96, is shown in Figure 2. The flux-density scale has been corrected for overlap between the beams: At a spacing of 3.'8 on a hexagonal grid, the effective forward gain of the summed beam is 1.6 times the gain of a single beam, as derived from detailed maps of the flat-feed beam and sidelobes (Corbelli, Schneider, and Salpeter 1989). The total integrated flux is 95 Jy km s^{-1}. This value can be compared to other smaller dish measurements by appropriately weighting the individual Arecibo beams to reproduce the gain pattern of the larger beam. A flux of 62 Jy km s^{-1} is predicted for the Green Bank 300 foot (91 m) telescope compared to 61 Jy km s^{-1} actually measured (Dickel and Rood 1978), and 84 Jy km s^{-1} for the Green Bank 140 foot (43 m) telescope compared to 112 Jy km s^{-1} measured (Fisher and Tully 1981).

The shape and symmetry of M96's profile is fairly typical of the double-horned structure found in spiral galaxies. Using the asymmetry index of Peterson and Shostak (1974), there is a 15% difference between the integrated flux in the high- and low-velocity halves of the profile, which is somewhat greater than the average of 5% found for late-type galaxies, but which is not particularly unusual based on an inspection of the H I profiles of other early-type galaxies (see, e.g., Huchtmeier 1982). Other single-dish observations show M96's profile to be flat-topped, lacking the normal two-horn rotational structure. This difference is a consequence of the beam size of the other instruments used. Observations made with the Green Bank 300 foot telescope suffer from a beam that is slightly too small for the galaxy. Gas 5′ from the center is only detected at the half-power level in the beam; thus, the outer parts of the galaxy, which contribute most to the velocity extremes, are underrepresented. The 21′ beam of the Green Bank 140 foot telescope also underrepresents the outer regions slightly, but more importantly the beam is so large that gas from the intergalactic

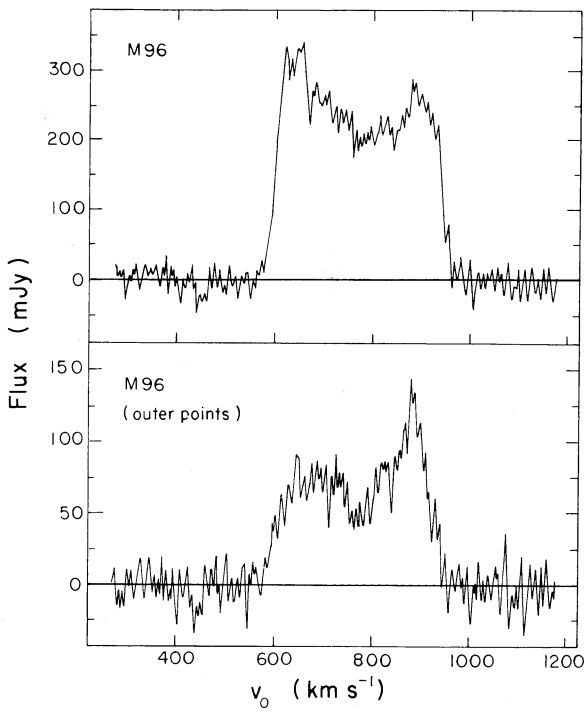

FIG. 2.—21 cm spectrum of the galaxy M96. The upper spectrum shows the summed emission from the inner 17 points in the hexagonal sampling pattern (see Fig. 3*a*), covering emission over a ~17′ diameter region centered on M96. The flux density scale has been corrected for the effective forward gain of the summed beam, and the rms about the baseline fit is 14 mJy. The lower spectrum shows the summed emission for the 12 points in a ring around the galaxy, covering emission between radii of ~6′ and 9′. The rms about the baseline fit is 11 mJy.

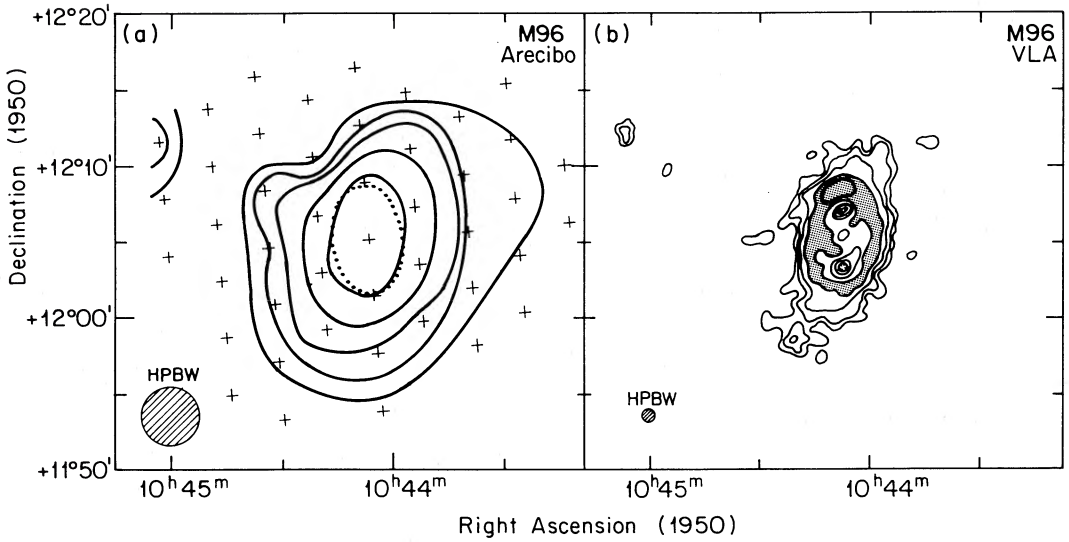

FIG. 3.—The distribution of neutral hydrogen in M96. (*a*) Integrated intensity of the H I mapped at Arecibo. Contours are marked for levels of 1, 2, 4, 8, and 16 × 10^{19} cm^{-2} (assuming 1 Jy km s^{-1} per beam corresponds to a column density of 10^{19} cm^{-2} for the Arecibo flat feed). A dotted ellipse marks the optical dimensions of the outer ring of optical emission, and crosses mark the points observed on the hexagonal grid. (*b*) Integrated H I intensity from VLA D-array observations. The contour levels are at 4, 8, 16, 32, and 64 × 10^{19} cm^{-2} (assuming 1 Jy km s^{-1} per beam corresponds to a column density of 4 × 10^{20} cm^{-2} for the synthesized VLA beam). The regions of highest H I column densities, forming a ring at the diameter of the outer optical ring, are shaded to avoid ambiguity in the contour levels. The H I column density declines in regions interior to the shaded ring.

cloud contaminates the spectrum, adding to the central portion of M96's profile and the measured flux (see above). By contrast, the summed Arecibo observations provide nearly uniform sensitivity across the entire disk of a large galaxy such as M96 without introducing confusion.

The most unusual aspect of M96's H I profile is that the maxima on either side of the profile are inset from the edges, closer to the systemic velocity of the galaxy. The lower spectrum in Figure 2 is the sum of the 12 outermost points included in the upper; it primarily samples the H I emission from a region between 6′ and 9′ from the center of M96. This spectrum shows that the outermost regions are the source of the lower velocity gas. The lower velocities may result from a declining rotation curve or a change to lower inclination in the outer parts of the galaxy.

A total intensity map of the H I distribution in M96 is shown in Figure 3*a*. The emission is fairly symmetric about the optical center of the galaxy. The asymmetries in Rots's (1980) map of M96 are apparently due to the "severe residual baseline curvature" he had encountered in making his Green Bank map. A shift in the center of emission in a velocity-position contour map made by Helou *et al.* (1981) and some slight asymmetries found in the present observations of M96, as well as M95 and NGC 3389 (see below), appear to be accounted for by the 20″–30″ pointing errors at Arecibo.

An extension from the main cloud of intergalactic gas enters the diagram northeast of M96, and a small opposed bump on the contours of M96 seems to point back toward it, but there is not evidently any direct connection to the galaxy—the intermediate point between the extension and galaxy shows virtually no emission. Moreover, the intergalactic extension is at a velocity of ~950 km s^{-1}, while the "bump" peaks at ~750 km s^{-1}. In addition, faint, narrow velocity-width H I at ~850 km s^{-1} is detected extending to the northwest of the galaxy.

a) VLA H I *Observations*

In Figure 3*b*, a D-array VLA map of M96 is shown. The 5 hr integration was made in 1984 October with 25 antennas and 31 channels, each 97.6 kHz wide (~21 km s^{-1}) in the center of a 6.25 MHz bandpass. On-line Hanning smoothing was used, and the synthesized beam was smoothed to be circular with a full width at half-maximum of 45″. Only minor cleaning was required. Regions not containing any apparent emission in the individual channel maps were blanked, and the moments were then calculated for the emission. The total H I flux detected in M96 was 62 Jy km s^{-1}, or roughly two-thirds of the total H I emission as observed at Arecibo. The missing one-third is probably in part undetected faint emission in the outer regions of M96 and in part some fraction of the H I distributed over the entire disk with too low a spatial frequency to be detected at the shortest interferometer spacings in the D-array.

In the VLA map the H I is seen to be concentrated in a distinct bright ring of emission (shown shaded in Fig. 3*b*), corresponding to the faint outer ring seen optically. The extension from the intergalactic cloud is resolved and is clearly distinct from any of the galaxy's emission. Weakly emitting H I surrounds the ring but was only partially visible at the level of noise in the individual channel maps.

From a map of the mean velocity structure (Fig. 4), it can be seen that the isovelocity contours become closed in the outermost parts of the galaxy, indicating that the H I is returning to more moderate velocities from the extremes in the bright emission of the ring (the approximate optical dimensions of which are shown with a dotted ellipse). This agrees with the interpretation of the inset peaks of the H I profile in Figure 2 and the narrow-line gas to the northwest in the Arecibo data discussed above. Based on the changing direction of the rotational major axis in the outer regions, it appears that the outer disk is warped.

The structure of the H I closely matches the outer optical ring in shape and extent, and, like the optical emission, the H I emission is stronger in the northern portion of the ring. However, relatively little H I emission is detected from the inner, optically bright part of the galaxy, and the angle of the

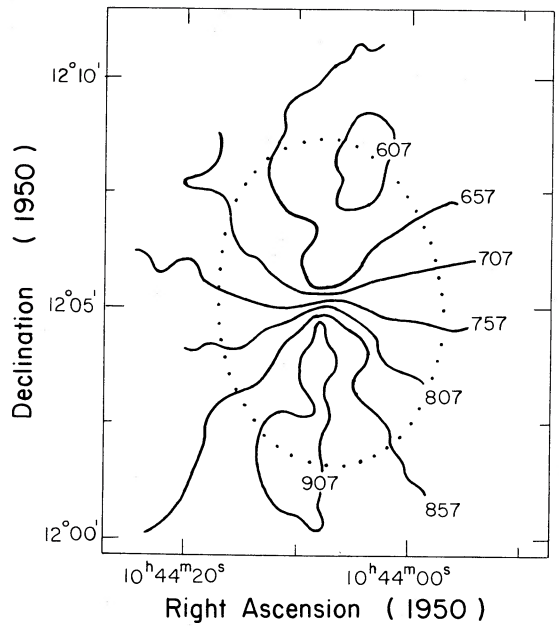

FIG. 4.—The velocity structure of the neutral hydrogen in M96. The flux-weighted mean velocity of M96 from the VLA observations is shown. Galactocentric velocities are marked. The mean Galactocentric velocity of M96 is 757 km s^{-1} from single-dish observations. The dotted ellipse marks the optical dimensions of the outer ring.

H I velocity contours in Figure 4 does not shift toward the interior of the galaxy to match the position angle of the inner disk, but just the reverse. A model of this H I emission as a warped disk by van Moorsel (1985) shows that the direction of the effective rotation changes from the outer parts of the ring to the inner in such a manner that the expected position angle in the inner regions would be nearly perpendicular to the apparent orientation of the optical disk.

Approximately 90% of the H I emission appears to be located outside of the bright optical disk of M96, mainly concentrated in the outer ring. The precise fraction is difficult to establish because of the H I that was undetected at the VLA; however, the undetected gas is presumably distributed over relatively large angular scales and would not add significantly to just the central region. Annular distributions of H I have been found in early-type galaxies from S0 to Sa studied by van Driel (1987), not all of which have a corresponding outer optical ring. Van Driel suggests that the H I in such rings may have been captured from other galaxies or intergalactic clouds. M96 is unusual in that a likely source for captured gas has been identified nearby. Of course, if the H I in the outer ring is captured, the original H I content of M96 must have been relatively low, perhaps less than 1% compared to the luminosity of the galaxy. This would place M96 originally among the Sa galaxies at the low end of H I content studied by Huchtmeier (1982).

The overall impression of the observations is of some level of disturbance in the outer parts of the galaxy, given the scattered faint H I beyond the outer ring and the warped outer disk. But there is no clear indication of the common sorts of tidal structures to suggest that the intergalactic gas might have been tidally removed from M96. Actually, the shape of the extension of intergalactic gas from the main cloud toward M96 suggests the reverse. The narrow tail of H I extending south from the intergalactic ring (Schneider, Salpeter, and Terzian 1986) is best explained by M96's tidal field pulling out gas from the ring as it orbits clockwise on the sky (Paper I). The origin of the intergalactic cloud in a Spitzer-Baade collision between M96 and NGC 3384 also appears to be at odds with the geometry and velocity structure of the intergalactic ring gas as it is now mapped (Papers I and II).

Without an optical determination of the rotational axis of the interior regions of M96, it remains unclear whether the outer region is rotating at a large inclination to the central disk, or whether the inner region is rotating with a strong oval distortion. An inclined outer ring is unstable and so is not normally expected to be found around a galaxy, but, in the present circumstance, with an external source of H I and evidence for interaction with the intergalactic gas, it is tempting to speculate that the outer ring represents a more recently formed structure produced by infall of intergalactic gas onto M96. On the other hand, the asymmetric appearance of dust absorption in the optical image of M96 may be evidence for an oval distortion in M96's inner disk.

IV. M95

Observations were also carried out for M95 (NGC 3351) at Arecibo in the same manner as for M96. M95 is an SB(r)b galaxy, which is undergoing mild starburst activity (Alloin and Nieto 1982) and is the only other large spiral galaxy in the M96 group. Its bar and internal structure have been studied in detail, and an inner ring of H II regions appears to be contracting (Rubin, Ford, and Peterson 1975; Peterson *et al.* 1976).

The composite Arecibo H I profile and H I distribution are presented in Figures 5 and 6. The H I profile was again produced by summing the spectra at points where H I was detected and correcting for the overlap. The integrated flux found is 48 Jy km s^{-1}. The predicted Green Bank 300 foot flux is 38 Jy km s^{-1}, compared to 36 Jy km s^{-1} (Peterson *et al.* 1976), 41 Jy km s^{-1} (Dickel and Rood 1978), and 45 Jy km s^{-1} (Shostak 1978). The predicted Green Bank 140 foot flux is 45 Jy km s^{-1}, compared to 55 Jy km s^{-1} (Peterson *et al.* 1976) and 50 Jy km s^{-1} (Shostak 1978). The Arecibo predicted fluxes appear slightly low relative to the Green Bank measurements, but they are

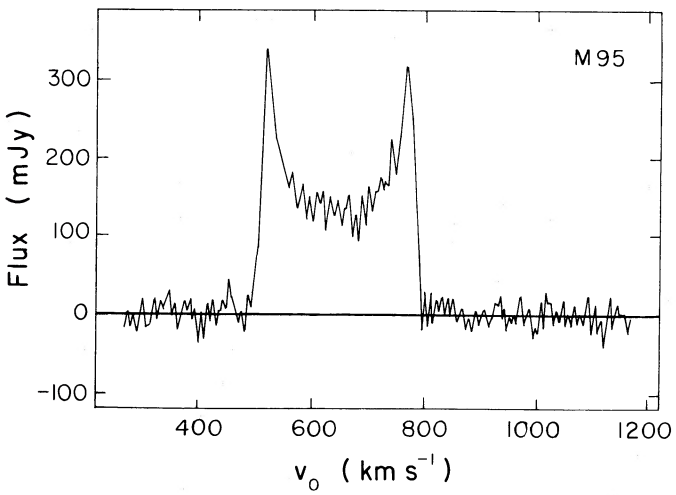

FIG. 5.—Arecibo H I profile of M95. The summed spectrum for the central 19 observed positions is shown, corrected for the effective forward gain of the summed beam as in Fig. 2.

within the range of possible calibration errors.

The H I characteristics of M95 are very symmetric both spatially and kinematically. The integrated flux of the H I is fairly normal for this galaxy's type as well. Giovanelli (1984) has commented, however, that in modeling the major axis distribution of H I in M95 he finds an unusually small extent relative to the Holmberg dimensions. This is also evident from the integrated emission (Fig. 6) in that the level at 50% of peak is reached already at the optical radius of the galaxy, and the emission drops off precipitously beyond this radius.

This small extent might appear to be suggestive of past tidal stripping of M95, and potentially a source for the intergalactic gas in the M96 group. Tidal stripping is unlikely, though, to have produced a more confined distribution of H I. The prograde tidal encounter that would be required to draw out large amounts of gas from the outer reaches of the galaxy would also impart excess angular momentum to the rest of the disk, thereby stirring up the gas. If anything, M95 seems more likely to have undergone a retrograde encounter that has shrunk down its disk, and that might conceivably account for its starburst activity. However, Alloin and Nieto (1982) suggest that the starburst began only a few $\times 10^7$ years ago, yet, given the high degree of symmetry observed, it seems that any tidal encounter would have to have taken place several galactic revolutions earlier.

V. NGC 3389 *et al.*

The final galaxy that was mapped at Arecibo is the SA(s)c galaxy NGC 3389. This galaxy is located on the sky near to M105 and NGC 3384, and together they are occasionally confused for the Leo Triplet farther east. de Vaucouleurs (1967), in studying a supernova in NGC 3389, concluded from it and several other aspects of the galaxy that rather than being a small, low-luminosity Sc in the M96 group, it is more likely background to the group. Application of the Tully-Fisher method also appears to support this view (de Vaucouleurs *et al.* 1981; and see below). However, NGC 3389's neutral hydrogen displays some peculiar features, and there is considerable uncertainty in the literature as to its distance, so that an examination of this galaxy in relation to the intergalactic gas was undertaken.

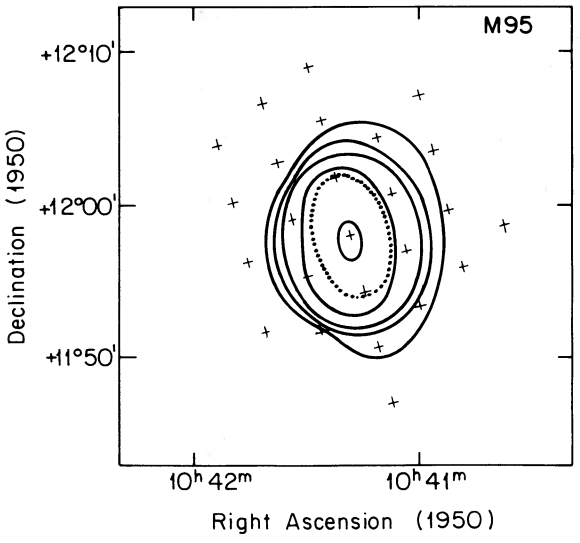

FIG. 6.—The H I distribution of M95, as in Fig. 3*a*. The optical dimensions of M95 are shown with a dotted line.

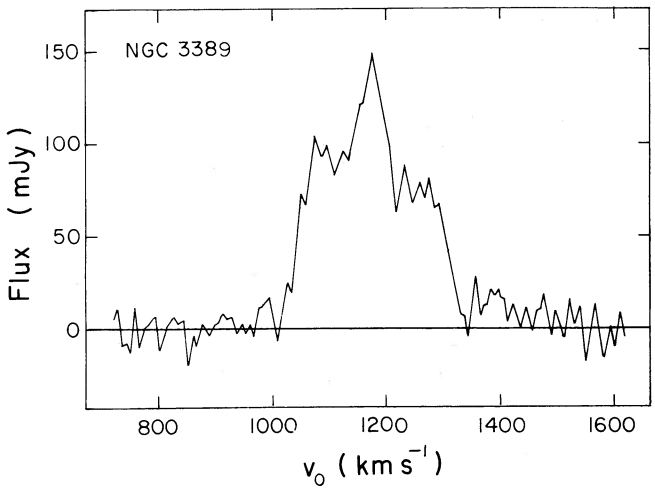

FIG. 7.—Arecibo H I profile of NGC 3389. Summed spectrum of the points observed as in Fig. 2.

NGC 3389 received limited mapping at Arecibo, but the central points around the galaxy were observed at a 1'.9 interval to study the structure in more detail. In addition, circular feed search spectra from other H I studies of the region (Papers I and II) covered NGC 3389's velocity range. Its 10% sidelobe makes the circular feed confusing for mapping extended emission, but it is possible to correct the observed fluxes. This was not particularly a problem around NGC 3389 because of the narrow H I lines encountered, and the geometry of the gas distribution.

NGC 3389 shows a peculiar central peak in its spectrum (Fig. 7). Gas at this velocity appears to continue southeast from the galaxy along its major axis. Features like this are usually indicative of tidal encounters or confusion. This initially appeared surprising, given the apparent lack of nearby galaxies if NGC 3389 is actually more distant than the M96 group. However, the search spectra also turned up three small galaxies in the vicinity with velocities similar to NGC 3389, which have also been examined by Hoffman *et al.* (1987). The faint galaxy Zw 066.029 was detected at 1380 km s^{-1} to the southeast of NGC 3389 (Fig. 8) and appears to be the most likely culprit to have caused the peculiar H I features. Zw 066.029 has an unusual morphology on the Palomar Sky Survey, and narrow-velocity H I features were detected extending away to the north of it. Hoffman *et al.* actually distinguish this dwarf into a pair with a separate optical feature corresponding to the northern tail of H I emission. Given the structure of NGC 3389's H I emission in relation to these galaxies, it appears likely that they are undergoing some type of tidal encounter, perhaps analogous to the Magellanic Clouds around our own Galaxy. The odd central peak in NGC 3389's H I spectrum can then be attributed to tidally stripped gas residing at a low systemic velocity around NGC 3389. Mrk 1263, detected farther south, bears no obvious distortions in its H I distribution and is probably not involved in this interaction, even though its velocity is similar.

Two other galaxies lying in the general neighborhood of the intergalactic ring were also examined to determine whether they might be members of the M96 group. An "off scan" of a search spectrum of UGC 5808 was the original source of the discovery of the intergalactic gas; UGC 5808 proves to be a

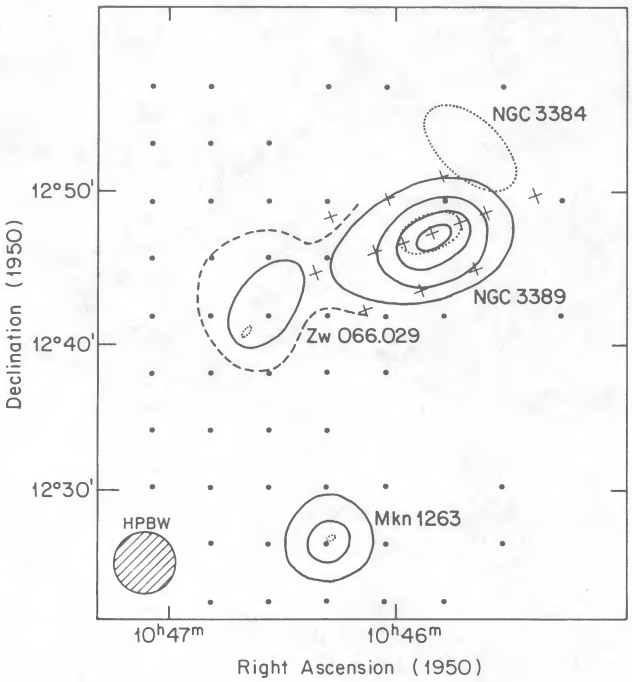

FIG. 8.—The distribution of H I around NGC 3389 and neighboring galaxies in the 1000 to 1400 km s^{-1} Galactocentric velocity range. Optical extents of the galaxies are shown with dotted lines. Crosses mark points observed with the Arecibo flat feed, and dots mark points observed with the dual-circular polarization feed. The contour levels are as in Fig. 3*a*, with the limits of detected emission shown by a dashed line.

face-on spiral at a much higher velocity of $v_{hel} = 7926$ km s^{-1} ($w_{50} = 39$ km s^{-1}, H I flux integral = 5.2 Jy km s^{-1}). A peculiar galaxy VIII Zw 105 at R.A.(1950) = $10^h46^m41^s$, decl. = +13°29′50″ lies along the ellipse of the intergalactic ring in the northernmost part where there is a gap in the H I. However, a spectrum obtained by Huchra (1988) shows it to be at a much higher redshift of 17,128 ± 36 km s^{-1}.

VI. LEO dw A: AN EXTREMELY FAINT DWARF

In the course of surveying the surroundings of the intergalactic cloud for the presence of more hydrogen (Paper II), a faint dwarf irregular galaxy was detected at R.A.(1950) = $10^h44^m14^s$, decl. = 13°00′20″. No object is visible at this position on the Palomar Survey Prints. Follow-up optical observations show that this is one of the faintest and lowest surface brightness dwarf irregulars yet recorded. For consistency with previous naming conventions, this dwarf is hereafter referred to as Leo dw A.

The nature of this object was suspected from the Arecibo observations because of its confinement to a single 3′.3 beam in the search grid. The dwarf lies nearly along the intergalactic ring as seen on the sky (Fig. 1), but its Galactocentric redshift is only $v_0 = 510$ km s^{-1}, which is significantly lower than any of the intergalactic gas.

Blue CCD observations (Fig. 9) were made at Kitt Peak, and a very low surface brightness object was detected less than 1′ from the Arecibo coordinates, which is within the positional uncertainties of the observing grid. Two exposures were made, each lasting 2400 s, with the RCA CCD on the No. 1 0.9 m telescope. Edge bias and trim, bias frame subtraction, and flat-field division were performed. The image was calibrated with stars in M67, using the broad-band magnitudes of Schild (1983), and had a background surface brightness of 22.0 mag

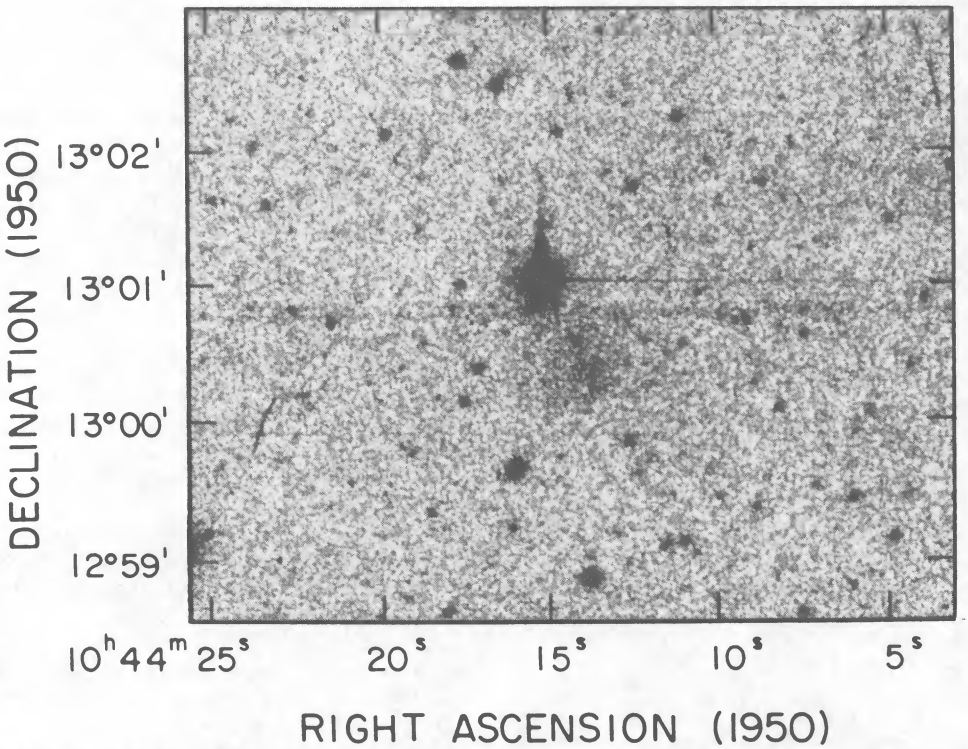

FIG. 9.—Blue CCD image of Leo dw A. The very low surface brightness dwarf irregular galaxy is visible near the center of this Kitt Peak image, just southwest of the central 15th magnitude star.

arcsec^{-2}(μ_B).

To determine its magnitude, the total counts from the dwarf were measured on each exposure, and average counts from several source-free regions were subtracted. The measurement was made difficult by a nearby 15th magnitude star and by variations in the background counts across the field, but the derived magnitudes were consistent in both frames: $m_B = 18.95$ and 18.89. The correction for extinction at this high Galactic latitude is only 0.05 (Burstein and Heiles 1984). A blue magnitude of 18.9 is adopted for the remainder of this discussion for the total luminosity of the dwarf out to its visible limits in the CCD image, which covers visible emission to lower surface brightnesses than is generally considered.

The dimensions of visible emission from the dwarf are $\sim$0.'85 $\times$ 0.'65 down to a limiting blue surface brightness of $\sim 28.5\mu_B$, and the dwarf has a mean surface brightness of $\sim 27\mu_B$ over this area. The central 0.'5 $\times$ 0.'2 region is slightly brighter, with a mean surface brightness of $\sim 26\mu_B$. Given these low values, it is not surprising that the galaxy was invisible on the Palomar Survey, which has a limit of $\sim 25\mu_B$ on the blue prints (de Vaucouleurs, de Vaucouleurs, and Corwin 1976).

Assuming Leo dw A is a member of the M96 group, at a nominal distance of 10 Mpc its absolute magnitude is -11.1, making it one of the faintest dwarf irregulars detected outside of the Local Group, and probably the lowest surface brightness dwarf irregular yet detected. By comparison, one of the faintest dwarf irregulars previously found, M81 dw A, also has an absolute magnitude of -11 (Sargent, Sancisi, and Lo 1983) but is readily visible on the Palomar sky survey. Of the Virgo dwarf irregular galaxies detected in H I by Hoffman *et al.* (1987), Leo dw A is fainter than all but one which has a visually estimated magnitude of 19 and a substantially higher surface brightness ($\sim 24.5\mu_B$) and absolute magnitude (assuming it is at the distance of the Virgo cluster).

Since Leo dw A is at a low redshift relative to the M96 group, it may well be a foreground object, with a fainter absolute magnitude still. The question of distances in the Leo region will be addressed more fully in the next section, but it is noted here that using a single source of distance estimates (Tully 1988) and assuming that Leo dw A is a foreground Leo dwarf, its distance should be 5.8 Mpc versus 4.3 Mpc for M81 dw A. The absolute magnitude of Leo dw A is then -9.9, while that of M81 dw A would climb to -11.6. Using Tully's 8.1 Mpc distance for the M96 group also yields a fainter value of -10.6 for Leo dw A.

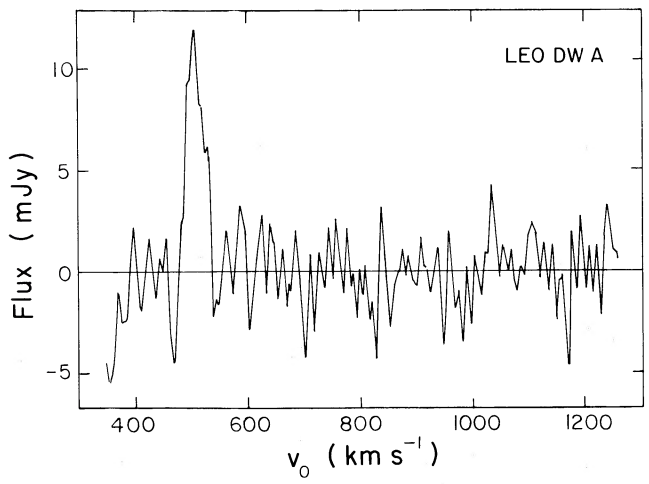

FIG. 10.—Arecibo H I profile of Leo dw A. The spectrum was taken with the Arecibo dual-circular feed.

The H I profile of Leo dw A (Fig. 10) has a velocity width at half-maximum of 29 km s^{-1}, which is not especially narrow compared to other faint dwarfs (Hoffman *et al.* 1987). The total H I mass is $8 \times 10^6\ M_\odot$, assuming the 10 Mpc distance, and about one-third of that using the 5.8 Mpc distance. There is some possibility of rotation, given the slight elongation of the image, but the profile does not show distinct rotation horns. The dynamical mass is $\sim 5 \times 10^7\ M_\odot$, based on the line width and optical size. Like M81 dw A and several of the fainter Virgo dwarf irregulars, the ratio of H I mass to blue luminosity in solar units for Leo dw A is somewhat greater than one. Dwarf irregular with much larger claimed values of $M_{\rm H\,I}/L_B$, such as CVn I dw A (Lo and Sargent 1979), are based on improbably low surface brightness estimates considering the plate material used.

The detection of such a faint galaxy by means of detailed mapping raises the possibility of searching for dwarf irregulars more widely via 21 cm mapping. The potential of finding faint galaxies with gas—possible precursors of star-bursting blue compact dwarfs—is intriguing, but difficult. To achieve a reasonable detection rate, one has the conflicting requirements of choosing a region with high galaxy density, both spatially and in velocity, yet not so high as in a cluster, where gas stripping is likely. The Leo region is relatively unique in both of these respects, in that the density of galaxies is high without an extensive hot intergalactic medium.

VII. THE LIMITS OF GROUPS AND GROUP-FINDING ALGORITHMS

Many authors have studied galaxy group membership in the Leo region and have reached widely different conclusions. The discussion of membership in the M96 group leads beyond the particulars of this region into a reexamination of the algorithms employed, their successes, and their failures with other groups as well. The M96 group proves to be one of the more difficult to select by objective criteria, which is in part a reflection of the complexity of the Leo region. But the problems found in defining the M96 group also apply to other groups and suggest that there may be extensive problems with group catalogs in general.

Several views have been forwarded regarding M96's group membership. The first is that essentially all Leo galaxies with velocities between 600 and 1300 km s^{-1} form a single large group (Sandage and Tammann 1975; Huchra and Geller 1982). Some have discerned between the M96 region and the Leo Triplet region, 10° to the east, but have maintained the large velocity range (Turner and Gott 1976; Geller and Huchra 1983). Still others have argued that the region is composed of many groups, with NGC 3389 and other higher redshift galaxies belonging to a more distant group $\sim$1.5 times more distant than the M96 group (Materne 1978; Tully 1987).

Methods using large redshift catalogs (Huchra and Geller 1982; Geller and Huchra 1983) find a large overdensity of galaxies in Leo that is not clearly divisible into smaller groups, yet this seemingly most objective method fails a simple test. The selection process results in an overabundance of faint, high-redshift galaxies in the groups. In particular, group 68 of Geller and Huchra contains M96 as its brightest galaxy, but of the 22 galaxies fainter than M96, 16 have higher redshifts. Such

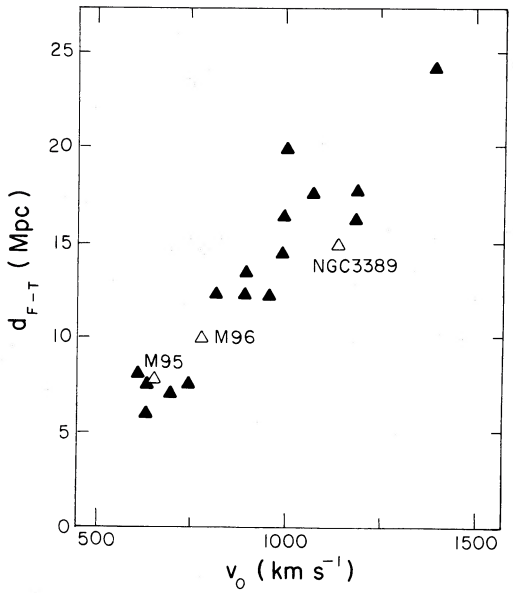

FIG. 11.—Fisher-Tully distances of M96 group candidates from the literature. The distances of the 19 spiral galaxies were scaled so that M96 would lie at its nominal distance of 10 Mpc.

a large asymmetry between higher and lower redshifts has a binomial probability of less than 3%.

In fact, many of the faint, higher velocity galaxies are farther away, based on independent estimators such as the Fisher-Tully distance. To demonstrate this point, a collection was made of all the Leo galaxies variously grouped together with M96: de Vaucouleurs (1975*a*), group 11; Sandage and Tammann (1975), Leo group; Turner and Gott (1976), group 27; Huchra and Geller (1982), group 56; Geller and Huchra (1983), group 68; Tully (1982), Leo I Cloud. Most of the 68 galaxies so listed were included by at least two authors. In Figure 11, the Fisher-Tully distance of spiral galaxies with H I measurements, with $v_0 < 2000$ km s^{-1}, and with inclinations larger than 30°, is plotted against the Galactocentric velocity. The distance scale in Figure 11 has been chosen so that M96 is at its nominal distance of 10 Mpc. The range of distances over which galaxies are found is ~20 Mpc. This is much greater than the projected diameter of the whole Leo region on the sky and its clearly much too large for these galaxies to all be dynamically associated.

All but four of the galaxies in Figure 11 are included in group 56 of Huchra and Geller (1982); seven are included in group 68 of Geller and Huchra (1983); and in both cases the velocity range over which the Fisher-Tully distances have been estimated is narrower than the velocity ranges of their proposed groups. Other distance estimators, like the magnitudes of galaxies in narrow ranges of luminosity classes, also show a clear increasing trend with velocity. Apparently, some group-finding methods are collecting together galaxies with large distance separations.

A contributing source to the problem is illustrated in Figure 12, which shows the distribution of the velocities of the galaxies over the entire (~20° diameter) Leo region centered at R.A.(1950) = 11^h, decl. = +12°, based on a compilation of velocities by Bicay (1987). A peak in the velocity histogram is seen near 1000 km s^{-1}, suggesting fairly strong clumping at this velocity. However, this peak is misleading.

The smooth curve in Figure 12 is based on a simple model with *no* assumed galaxy grouping, showing that the highly peaked distribution is consistent with the galaxies being spread uniformly over a large range of distances. The source of the peak in the velocity distribution is deviations in the Hubble flow induced by the Virgo Cluster. Between 15° and 25° from Virgo, where most of the Leo galaxies lie, the redshift increases rapidly out to ~12 Mpc and then changes slowly or lessens out to ~20 Mpc before increasing again (for a distance of 18 Mpc to Virgo), causing the Leo galaxies to bunch near the redshift of Virgo. The velocity crowding has misled many of the attempts to find groups in this region.

The group-finding methods that work best in this difficult Leo region are based on the hierarchical method first suggested by Materne (1978), who applied the method to the Leo region and distinguished a number of foreground and background groups. Huchra and Geller (1982) fault Materne's attempt for arriving at velocity dispersions too low to be physically reasonable, yet Materne is more successful in separating what must be independent galaxies based on the preceding discussion. The algorithm used by Huchra and Geller might be improved in the Leo region by recognizing the effects of velocity crowding when setting their velocity cutoff, but it is not the Leo region alone which presents problems for their method.

There is also evidence that even the smaller, non-Leo groups in Geller and Huchra (1983) are contaminated with background galaxies. Like their Group 68, groups with 10 or fewer members suffer from a bias, with the faint members tending to have larger redshifts than the brightest galaxy. Of 566 fainter companions in these groups, 326 (57.6%) are at higher redshifts, which has a binomial probability of less than 2×10^{-4}.

Gravitationally bound galaxies should show no such asymmetry since the sign of the orbital velocity difference is arbitrary whatever the projected separation on the sky, but the number of "interloping" (foreground or background) galaxies depends on the shape of the region searched for companions. Like most group-finding methods, the Geller and Huchra algorithm uses angular and velocity-difference cutoffs, resulting in a

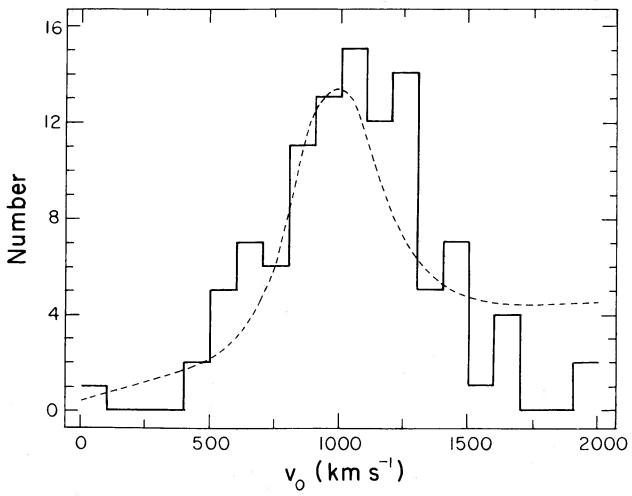

FIG. 12.—Histogram of all published galaxy velocities in the Leo region under 2000 km s^{-1}. The smooth dashed curve is a model assuming a uniform distribution of the galaxies with distance, but including the effects of velocity crowding caused by Virgocentric deviations from the Hubble flow.

search region which is essentially a truncated cone with its base at the high-velocity cutoff. Comparing the volumes of the low-velocity half to the high-velocity half of this search region for each of the Geller and Huchra (1983) groups (using twice the velocity dispersion of each group as a measure of the depth of the cone), one would predict that ~56% of interloping galaxies should have higher redshifts.

The implication of this simple model, which does not account for distance-dependent selection biases within the search regions, is that *all* of the Geller and Huchra groups would have to result from interlopers to begin to explain the 57.6% of higher redshift galaxies. It must be noted that the number of such incidental groupings should be nowhere near this large, based on the expected number of interlopers from averages over the whole CfA sample; however, the effects on their algorithm of velocity crowding associated with large-scale structure in the universe is not so clear. Sulentic (1984) and Byrd and Valtonen (1985) have attempted to explain this asymmetry with more fully developed alternative models, but here it is simply noted that there are genuine concerns about the reality of the groupings as listed. At the very least, estimates of group virial masses must be regarded as suspect, and individual memberships must be placed in some doubt.

Huchra and Geller (1982) justify their large velocity dispersions by arguing that otherwise the crossing times would be long relative to a Hubble time, and the groups would not then be virialized. However, this rationale cannot be used to validate their groups since they define the crossing time in terms of the *angular* separation divided by the *line-of-sight* velocity dispersion, and they have chosen to accept large velocity differences. Given the problems encountered, it appears necessary to argue that galaxy groups actually do have long crossing times and may not be virialized. In some sense, then, they would not be groups at all, but perhaps temporary associations of unbound galaxies. Rivolo and Yahil (1981) find that the velocity dispersion seen between neighboring galaxies is consistent with the general galaxian dispersion, and they argue that a large fraction of binary galaxies are also either foreground/background pairs or temporary associations. If many groups are only weak associations, decelerated with respect to the Hubble flow but not yet virialized, their line-of-sight velocity differences could be even smaller than those predicted from the universal expansion, and their apparent crossing times might appear larger than for even random collections of galaxies in the field. This line of argument ultimately suggests that either virialization has not taken place and the mass estimates are inapplicable, or that groups of galaxies are much less massive than determined from catalogs of groups that accept these problematic large velocity differences—a conclusion that complements what is shown for the M96 group next.

VIII. THE M96 GROUP AND THE INTERGALACTIC RING

For the M96 group the radical question might be raised: do any of the galaxies form a dynamical, gravitationally bound group? After all, Figures 11 and 12 indicate that the galaxies in the region may be spread evenly over a large range of distances. Even if a diameter for the M96 group as large as 10° is accepted, the depth of the group should be on the order of only 1.7 Mpc (at a distance of 10 Mpc). In Figure 11, NGC 3389 is clearly at a larger distance and higher velocity, and even M95, a galaxy attributed to the M96 group by every author listed in the previous section, has a smaller Fisher-Tully distance as well as a smaller velocity. Perhaps M95 should instead be associated with the Leo Triplet galaxies 10° to the east. Where can the line be drawn?

In the M96 group, the ring of intergalactic gas provides a unique opportunity to probe the mass distribution in a group, well beyond the optical disks of the galaxies. A Keplerian model of the ring orbit predicts the position and velocity of the central galaxies *without any additional assumptions* (Papers I and II). The model finds the presence of a gravitating mass of $6.4 \times 10^{11}\ M_\odot$ with a center-of-mass velocity of $v_0 = 700$ km s^{-1} at a position near to the galaxies M105 and NGC 3384, a giant elliptical and a lenticular forming a pair. Remarkably, the 700 km s^{-1} velocity also nearly matches the center-of-mass velocity of this same pair of galaxies, which are suspected close companions based on detailed optical observations (Nieto and Vidal 1984). This mass is only a factor of 2 greater than the mass estimates of the pair based on their internal velocity dispersions (Tonry and Davis 1981) and gives a modest mass-to-light ratio of $M/L = 27$ (in solar units) for the total mass distribution out to ~100 kpc beyond their optical limits. The position and velocity of the ring's center of mass also match well with the values for the entire M96 group described by de Vaucouleurs (1975*a*), Materne (1978), or Tully (1988). Thus the ring "predicts" the location and mass of the center of the M96 group and "finds" the central galaxies.

In addition, minor deviations from the orbit of gas on the periphery of the ring and a small apparently tidal tail pulled out of the ring indicate an interaction with M96. Thus the ring directly links the galaxies M96, M105, and NGC 3384, and it further provides a means of testing other likely group members. Using the mass implied by the ring, an escape velocity of 153 km s^{-1} $= (2GM/R)^{1/2}$ is indicated for the projected separation of M95 from the dynamical center of the ring compared to a measured velocity difference of 51 km s^{-1}. Of course, this is at best a rough guide to whether a galaxy might be bound, since the total group mass interior to M95 is presumably greater, while the three-dimensional velocity difference and the spatial separation are almost certainly larger than their projected values. However, even if M95 were separated along the line of sight by a distance implied by the Hubble flow, the observed velocity difference is still smaller than the escape velocity. It therefore seems likely that the distance difference suggested by Figure 11 is the result of the intrinsic dispersion in the Fisher-Tully relation and that M95 is indeed associated with the M96 group. Likewise, M96, M105, NGC 3384, and NGC 3412 all have velocity differences of between one-fifth and one-third the escape velocity for their projected separations from the ring center and are fairly definite members of the M96 group.

One traditional member of the M96 group, NGC 3377, as well as NGC 3389, NGC 3299, DDO 88 (UGC 5889), and UGC 5812, have velocity differences approximately equal to or greater than the escape velocity calculated for their projected separations. Thus, these galaxies may not be bound to the M96 group unless the projection effects work in their favor or the interior mass is greater. For NGC 3389, the independent distance estimators discussed earlier confirm that it is most likely a background galaxy, but NGC 3377, an elliptical, DDO 88 and UGC 5812, both dwarfs, and NGC 3299, a face-on galaxy, do not have any other sufficiently accurate distance estimates to decide the issue.

Leo dw A is an important case, since a smaller distance places it at the extreme low end of the galaxy luminosity func-

tion. Its velocity difference from the center of mass of the ring is 191 km s^{-1} which is 61% of the escape velocity at its projected separation of 55 kpc, so that it could be a bound member of the group if its projected separation and velocity difference are the actual values. Since it would then lie inside of the ring orbit, no extra mass can be called upon to help argue for its inclusion in the group. The probability of the projection effects allowing it to be in a circular orbit with its observed velocity difference is ~20%, so that its inclusion in the M96 group remains uncertain.

The velocity dispersion of the five most definite members of the M96 group is 82 km s^{-1}—much smaller than the 234 km s^{-1} found by Geller and Huchra (1983). However, following their development and despite the smaller dispersion, a crossing time of only 4% of the Hubble time is found (as opposed to their 5%), which still suggests that this group, in its more limited definition, has had time to become virialized. The virial mass of the group based on these five galaxies, again following Geller and Huchra, is $7.7 \times 10^{11}\ M_{\odot}$, slightly greater than the mass implied by the ring orbit, but considerably more uncertain. The luminosity of these five galaxies totals to $6.5 \times 10^{10}\ M_{\odot}$, resulting in an M/L ratio of ~12. Including some of the less certain members of the group, such as NGC 3377, would approximately double the virial mass estimation, bringing M/L more in line with the value indicated by the intergalactic ring for the central two galaxies. This is still much lower than the M/L value of 205 found by Geller and Huchra for Group 68. Large M/L values of 400 (Mezzetti *et al.* 1985) and 630 (Heisler, Tremaine, and Bahcall 1985), based on averages of the Geller and Huchra groups, are probably inflated by interlopers, too.

The short crossing time in the M96 group results in a puzzle about the ring of intergalactic gas. The presence of gas at points all around the orbit suggests that it must have existed for at least one full revolution, or $\sim 4 \times 10^9$ yr (Paper I). If the gas was injected into its orbit by some tidal event, it is difficult to imagine any way of spreading it around the ellipse via differential rotation in less than a few orbital periods. This length of time approaches a Hubble time, and many group crossing times, so that in its central location, the ring should have suffered many close collisions if the orbits of the galaxies are randomly oriented.

Tidal modeling of such collisions was performed, in the manner of the Toomre and Toomre (1972) models, which are almost ideally suited to the physical circumstances of the ring. The results suggest that massive galaxies in orbits crossing closer than twice the radius of the ring orbit would have dramatic disruptive effects. M96 currently appears to be passing at twice the ring orbit radius, which brings gas on the periphery of the ring into its sphere of influence, and may thereby account for the tidal-looking feature extending toward it from the southern part of the ring. A large number of closer collisions would probably destroy the ring entirely.

The best way to reconcile the regular structure of the ring and the short crossing time for the group would be if the galaxies in the group remained at large distances from the ring on low eccentricity orbits. If NGC 3377 is also included, there appears to be a trend, on average, in the group member's velocities from northeast to southwest that is similar to the trend of measured velocities in the intergalactic ring. This could mean that the ring and the whole M96 group are rotating in roughly the same sense, although the individual deviations of the velocities of the galaxies are too large to suggest that their orbits are very near to being coplanar. Of course, such a pattern of rotation could wreak havoc with virial estimates, but fortunately the ring's orbit model suggests that the group would be included by ~45° to the line of sight, so the estimates should not be far off. This model would also be consistent with a primordial origin of the intergalactic cloud, as residual material left over from the formation of the whole group.

M96 may be directly responsible for shaping the ring, by orbiting at twice the ring's radius and stripping off the outermost gas during near encounters. The numerical simulations indicate that if M96 were always present at twice the radius, the intergalactic ring would lose much of its mass to M96 and be largely disrupted, but if its orbital plane were inclined to the ring's, the destruction would be lessened. The relative velocities of the ring and M96 also suggest that their orbital planes are different: The velocity of gas in the ring, at the position angle of M96 relative to the ring's center of mass, is ~3 times greater than that of M96 at about half the radius. A Keplerian falloff would not yield this large a change, but an inclination of 23° between their orbital planes could account for the difference.

The present edge of the ring orbit, at almost precisely the halfway point on a line joining M96 and the ring's center of mass, is probably a consequence of the weak dependence of the radius of the sphere of influence on mass. Only ring gas at distance from M105 and NGC 3384 greater than its distance to M96 by a factor greater than

$$[\text{Mass(M105 + NGC 3384)/Mass(M96)}]^{1/3} \approx 1.18$$

will fall into M96's sphere of influence. The close passages of M96 on an inclined orbit would be rare, occurring twice in its $\sim 10^{10}$ yr orbit, but perhaps adequate to help define the outer limits of the ring. In this scenario, the other galaxies would remain on orbits sufficiently far away that they would not significantly influence the ring, which appears to be consistent with their individual velocities.

IX. SUMMARY

Neutral hydrogen observations of the M96 group provide insight into the nature of the ~200 kpc diameter ring of intergalactic gas and its relationship to the nearby galaxies. Synthesis-array and single-dish observations of the neutral hydrogen in M96 suggest that it is interacting with the ring, and perhaps drawing off gas to feed its own faint outer optical ring. It seems improbable that many other galaxies with faint outer rings have a similar external source for their origin, but it is not clear that present observations have exhausted this possibility.

The observations of the ring at 21 cm also revealed an extremely faint dwarf irregular galaxy in the Leo region. The absolute magnitude of this galaxy is one of the faintest yet observed outside of the Local Group. High-sensitivity searches with complete coverage at 21 cm could provide a valuable means in the future for finding more faint galaxies which have not yet undergone the burst of star formation that is usually needed to locate them optically, although the space density of such objects may be too low to achieve reasonable detection rates.

The wide discrepancies in claimed group membership in the Leo region show that there must be problems with many of the group-finding algorithms used. Since derived quantities such as virial masses of groups are intimately tied to the choice of their boundaries, it is imperative that alternative means be

used to confirm the groupings. In the nearby M96 group, independent distance estimators narrow the possibilities to a much more limited group membership then in Geller and Huchra (1983). There are hints of similar discrepancies in other cataloged groups, suggesting that the problem of inflated virial masses may be widespread.

Finally, the orbital dynamics of the intergalactic ring and the group membership indicated by its presence both indicate that the mass-to-light ratio of the M96 group is less than 30. This is an order of magnitude smaller than some previous estimates and not very much greater than the mass-to-light ratios derived internally for the individual galaxies, which suggests that there is not a large amount of dark matter between the galaxies. The intergalactic cloud might itself be termed "dark matter" since it is underluminous by a factor of more than 10 compared to even its neutral hydrogen mass (Paper II), but it does not contribute much to the total dynamical mass of the group. Thus, perhaps ironically, the detected "dark matter" in the M96 group provides some of the most direct dynamical evidence yet for the lack of dark matter—at least to the extent supposed by many—in one group of galaxies.

I would like to thank Ed Salpeter, Yervant Terzian, Trinh Thuan, and Riccardo Giovanelli for valuable discussions. I also thank Vesa Junkarinen for obtaining the Kitt Peak CCD frame under the request observing program, John Huchra for determining the redshift of VIII Zw 105, and Mike Bicay for sharing his compilation of galaxy velocities.

APPENDIX

OPTIMIZED TWO-DIMENSIONAL SAMPLING

In mapping a region on the sky with a radio telescope, generally only a single point is observed at a time, and only low resolutions are available because of the long wavelengths involved. Some confusion is found in the literature regarding the necessary and sufficient degrees of sampling for one- and two-dimensional mapping with single-dish instruments.

The fundamental discourse on sampling date back to Bracewell and Roberts (1954) for one dimension, and to Bracewell (1956) for two dimensions. They phrased the question in terms of the telescope's spatial frequency coverage or u, v response pattern. The highest spatial frequency that is detectable (corresponding to the smallest resolvable structure) is determined by the illuminated diameter of the dish. In a more general treatment, it can be shown that some higher spatial frequency information is present, but it drops off exponentially (Lo 1961), so that in the presence of noise, the Bracewell criterion is adequate.

The telescope's u, v response pattern must be convolved with the Fourier transform of the sky-sampling pattern to determine whether aliasing occurs. The largest spacing interval that avoids any aliasing of the u, v pattern is the *full-sampling interval*; smaller spacings needlessly oversample in that no higher spatial frequency information can be obtained, while larger spacing will lose some of the higher frequency information to aliasing.

A second important spacing interval is for *complete coverage*, in which not all of the spatial frequency information is obtained, but the total emission is detected. This requires that the spatial sum of the telescope beams at all of the observing positions yields an essentially uniform response on the sky. This might seem a complicated function of beam shape sidelobe structure, but in the spatial frequency domain, complete coverage is effectively a measurement of the zero-frequency (DC) component. Therefore, the spacing interval should not be so large that the zero-spacing frequency component becomes aliased. This requires that the convolution of the spatial pattern with the u, v response pattern not overlap by more than half. Complete coverage is therefore obtained at precisely twice the full-sampling interval.

One-dimensional sampling at a regular interval s along a line can be represented by a series of δ-functions along the x-axis, also known as a Ш (the letter *shah* from the cyrillic alphabet) or "picket fence" function,

$$Ш(x/s) = 1/\sqrt{s}\ \Sigma\delta[x/(s-n)]\ ,$$

where the sum is over all integers n.[4] The Fourier transform of this pattern is another Ш function in the u-coordinate: $F[Ш(x/s)] = Ш(us) = Ш(u/t)$, where $t = 1/s$ is the spatial frequency corresponding to the interval s. To meet Bracewell's full-sampling criterion, it is required that $t \geq 2d/\lambda$, where d is the diameter of the illumination pattern, and λ is the wavelength being observed, so that the full-sampling interval is $s_{fs} = \lambda/(2d)$.

The rule of thumb "half-beam spacing" is not necessarily a good choice for the sampling interval, since it may over- or underestimate the correct full-sampling interval, depending on the taper of the illumination pattern. For the 210 m diameter illumination pattern the Arecibo line feeds, the full-sampling interval is 1.'7 at 21 cm, whether the circular polarization (HPBW = 3.'3) or linear polarization ("flat") feed (HPBW = 4.'0) is used. Some consideration might also be given to the degree of tapering of the illumination pattern, since a strong taper may effectively limit the extent of spatial frequency coverage in the presence of noise, and no significant aliasing will occur unless very strong fluctuations are present in the spatial frequency distribution of the radiation being sampled. Conversely, the effects of pointing errors and a truncated sampling pattern (most do not extend to infinity!) will be to smear out the pattern-convolved u, v response function slightly, so that aliasing might still occur at the nominal full-sampling interval.

For a rectangular grid of observations, the previous discussion remains applicable since the grid pattern and its Fourier transform can be factored into orthogonal components. The Fourier transform of a square grid with spacing s is $F[Ш(x/s)\ Ш(y/s)] =$

[4] The factor of $1/s^{1/2}$ in the definition of Ш is introduced to symmetrize the functional form of the Fourier transform; the normalization of the function is otherwise unimportant in this discussion.

$\text{Ш}(u/t)\text{Ш}(v/t)$, where $t = 1/s$ as in the one-dimensional case.

More efficient coverage is possible in two dimensions, though. Closest packing of circles leads to a hexagonal or "honeycomb" pattern, not a rectangular one. For a hexagonal pattern $P_{\rm hex}$ in the (x, y)-plane, with spacing interval s, the points can be separated into two groups consisting of every other row, so that the entire pattern can be described as the sum of two rectangular grids:

$$P_{\rm hex} = \text{Ш}(x/s)\,\text{Ш}(y/\sqrt{3}s) + [\text{Ш}(2x/s) - \text{Ш}(x/s)]\,[\text{Ш}(2y/\sqrt{3}s) - \text{Ш}(y/\sqrt{3}s)]\,,$$

The Fourier transform of this pattern is

$$F[P_{\rm hex}] = \text{Ш}(v/t)\,\text{Ш}(u/\sqrt{3}t) + [\text{Ш}(2v/t) - \text{Ш}(v/t)][\text{Ш}(2u/\sqrt{3}t) - \text{Ш}(u/\sqrt{3}t)]\,,$$

where now $t = 2/(3^{1/2}s)$. This is of the same form as $P_{\rm hex}$ but rotated with the roles of u and v correspond to those of y and x, respectively. The full-sampling interval $s_{\rm hex}$ is larger by a factor of $2/3^{1/2}$ than in the rectangular case: $s_{\rm hex} = \lambda/(3^{1/2}d)$, or 1.96 for the Arecibo 21 cm feeds. The total increase of coverage for an equal number of positions is also $2/3^{1/2} = 1.15$, a 15% increase in coverage with no further loss of spatial frequency information.

In a large mapping project, using the hexagonal pattern presents more difficulties in cataloging and handling the data than does a rectangular pattern, but the advantages are also several. Although it is less than the one-dimensional full-sampling interval, an interval of $s_{\rm hex}$ may be used along the major axis of a galaxy for more rapid observations with the knowledge that if anything out of the ordinary is found, the data points can be used in a fully sampled two-dimensional map made subsequently. Furthermore, although most contouring programs are set up for rectangular grids, interpolation routines work best with data points at the vertices of equilateral triangles. (This is particularly obvious for saddle point structures in rectangular data.) Cataloging can also be handled reasonably well by basing x and y indices on a more extensive rectangular grid with $\Delta x = s_{\rm hex}/2$ and $\Delta y = 3^{1/2}s_{\rm hex}/2$, of which the hexagonal pattern makes up every other point. And, of course, for a large mapping project, the increased effective coverage corresponds to a 15% savings of valuable telescope time.

REFERENCES

Alloin, D., and Nieto, J.-L. 1982, *Astr. Ap. Suppl.*, **50**, 491.
Bicay, M. D. 1987, private communication.
Bracewell, R. N. 1956, *Australian J. Phys.*, **9**, 297.
Bracewell, R. N., and Roberts, J. A. 1954, *Australian J. Phys.*, **7**, 615.
Burstein, D., and Heiles, C. 1984, *Ap. J. Suppl.*, **54**, 33.
Byrd, G. G., and Valtonen, M. J. 1985, *Ap. J.*, **289**, 535.
Corbelli, E., Schneider, S. E., and Salpeter, E. E. 1989, *A.J.*, **97**, 390.
de Vaucouleurs, G. 1967, *Astrofizika*, **3**, 571.
———. 1975*a*, in *Stars and Stellar Systems*, Vol. **9**, *Galaxies and the Universe*, ed. A. Sandage, M. Sandage, and J. Kristian (Chicago: University of Chicago Press), p. 557.
———. 1975*b*, *Ap. J. Suppl.*, **29**, 193.
de Vaucouleurs, G., and de Vaucouleurs, A. 1964, *Reference Catalogue of Bright Galaxies* (Austin: University of Texas Press).
de Vaucouleurs, G., de Vaucouleurs, A., and Corwin, H. G., Jr. 1976, *Second Reference Catalogue of Bright Galaxies* (Austin: University of Texas Press).
de Vaucouleurs, G., Peters, W. L., Bottinelli, L., Gouguenheim, L., and Paturel, G. 1981, *Ap. J.*, **248**, 408.
Dickel, J. R., and Rood, H. J. 1978, *Ap. J.*, **223**, 391.
Dickson, R. J., and Hodge, P. W. 1981, *A.J.*, **86**, 826.
Fisher, J. R., and Tully, R. B. 1981, *Ap. J. Suppl.*, **47**, 139.
Geller, M. J., and Huchra, J. P. 1983, *Ap. J. Suppl.*, **52**, 61.
Giovanardi, C., Krumm, N., and Salpeter, E. E. 1985, *A.J.*, **88**, 1719.
Giovanelli, R. 1986, private communication.
Heisler, J., Tremaine, S., and Bahcall, J. N. 1985, *Ap. J.*, **298**, 8.
Helou, G., Giovanardi, C., Salpeter, E. E., and Krumm, N. 1981, *Ap. J. Suppl.*, **46**, 267.
Hoffman, G. L., Helou, G., Salpeter, E. E., Glosson, J., and Sandage, A. 1987, *Ap. J. Suppl.*, **63**, 247.
Huchra, J. P. 1988, private communication.
Huchra, J. P., Davis, M., Latham, D., and Tonry, J. 1983, *Ap. J. Suppl.*, **52**, 89.
Huchra, J. P., and Geller, M. J. 1982, *Ap. J.*, **257**, 423.
Huchtmeier, W. K. 1982, *Astr. Ap.*, **110**, 121.
Knapp, G. R., Kerr, F. J., and Williams, B. A. 1978, *Ap. J.*, **222**, 800.
Lo, K. Y., and Sargent, W. L. W. 1979, *Ap. J.*, **227**, 756.
Lo, Y. T. 1961, *J. Appl. Phys.*, **32**, 2052.
Materne, J. 1978, *Astr. Ap.*, **63**, 401.
Mezzetti, M., Pisani, A., Giuricin, G., and Mardirossian, F. 1985, *Astr. Ap.*, **143**, 188.
Nieto, J.-L., and Vidal, J.-L. 1984, *Astr. Ap.*, **135**, 190.
Nilson, P. N. 1973, *Uppsala General Catalog of Galaxies* (*Uppsala Astr. Obs. Ann.*, **6**).
Peterson, C. J., Rubin, V. C., Ford, W. K., Jr., and Thonnard, N. 1976, *Ap. J.*, **208**, 662.
Peterson, S. D., and Shostak, G. S. 1974, *A.J.*, **79**, 767.
Rivolo, A. R., and Yahil, A. 1981, *Ap. J.*, **251**, 477.
Rots, A. H. 1980, *Astr. Ap. Suppl.*, **41**, 189.
Rubin, V. C., Ford, W. K., Jr., and Peterson, C. J. 1975, *Ap. J.*, **199**, 39.
Sandage, A. 1961, *The Hubble Atlas of Galaxies* (Washington, DC: Carnegie Institution of Washington).
Sandage, A., and Tammann, G. A. 1975, *Ap. J.*, **196**, 313.
Sargent, W. L. W., Sancisi, R., and Lo, K. Y. 1983, *Ap. J.*, **265**, 711.
Schanberg, B. C. 1973, *Ap. J. Suppl.*, **26**, 115.
Schild, R. E. 1983, *Pub. A.S.P.*, **95**, 1021.
Schneider, S. E. 1985, *Ap. J. (Letters)*, **288**, L33 (Paper I).
Schneider, S. E., Helou, G., Salpeter, E. E., and Terzian, Y. 1983, *Ap. J. (Letters)*, **273**, L1.
———. 1986, *A.J.*, **92**, 742.
Schneider, S. E., Salpeter, E. E., and Terzian, Y. 1986, *A.J.*, **91**, 13.
Schneider, S. E., *et al.* 1989, *A.J.*, **97**, 666 (Paper II).
Shostak, G. S. 1978, *Astr. Ap.*, **68**, 321.
Sulentic, J. W. 1984, *Ap. J.*, **286**, 442.
Toomre, A., and Toomre, J. 1972, *Ap. J.*, **178**, 623.
Tonry, J. L., and Davis, M. 1981, *Ap. J.*, **246**, 666.
Tully, R. B. 1982, *Ap. J.*, **257**, 389.
———. 1987, *Ap. J.*, **321**, 280.
———. 1988, *Nearby Galaxies Catalog* (Cambridge: Cambridge University Press).
Turner, E. L., and Gott, J. R. 1976, *Ap. J. Suppl.*, **32**, 409.
van Driel, W. 1987, Ph.D. thesis, University of Groningen.
van Moorsel, G. 1985, private communication.

STEPHEN E. SCHNEIDER: 632 Lederle Tower, Astronomy Program, University of Massachusetts, Amherst, MA 01003